

# Core-shell SiO<sub>2</sub>/Ag composite spheres: synthesis, characterization and photocatalytic properties

ZHI GANG WU\*, YAN RONG JIA, JIAN WANG, YANG GUO, JIAN FENG GAO

Department of Chemistry, School of Science, North University of China, Taiyuan, 030051, Shanxi Province, P.R. China

Core-shell SiO<sub>2</sub>/Ag composite spheres with dense, complete and nanoscaled silver shell were prepared by using a novel facile chemical reduction method without surface modification of silica at room temperature. The core-shell composites were characterized by X-ray powder diffraction (XRD), scanning electron microscopy (SEM), UV-Vis spectroscopy and energy dispersive X-ray spectroscopy (EDX). The photocatalytic properties towards the degradation of methyl orange (MO) of the prepared SiO<sub>2</sub>/Ag composites were also tested. The studies showed that the surface of SiO<sub>2</sub> microspheres was homogeneously and completely covered by Ag nanoparticles and the composite exhibited excellent photocatalytic activities. The possible reaction mechanisms for the formation of the silica-silver core-shell spheres were also discussed in this paper.

Keywords: *core-shell; SiO<sub>2</sub>/Ag composite; deposition; photocatalytic property*

© Wrocław University of Technology.

## 1. Introduction

During the past decades, the design and controlled preparation of core-shell composites have attracted considerable attention and become an important research field in materials science, chemistry, medicine, and engineering [1–5]. Among the numerous kinds of core-shell structured materials, silica-silver structures consisting of silica cores and silver shells have been of significant interest because of their unique properties and potential applications ranging from optical devices and surface-enhanced Raman scattering to catalysis and medicine [6–9]. To date, there has been much effort on the synthesis of SiO<sub>2</sub>/Ag core-shell composites, including chemical reduction method, template, micro-emulsion method, layer by layer (LBL), sol-gel method, thermal deposition, and so on [10–15]. However, SiO<sub>2</sub>/Ag composites with dense, complete, uniform nanoscaled silver layer and high purity are still difficult to be obtained. Moreover, the fabrication process of the SiO<sub>2</sub>/Ag core-shell spheres generally involves a complex, time-consuming multi-step procedure. So, it is of great

interest to develop a simple and easy-handling procedure for the fabrication of SiO<sub>2</sub>/Ag core-shell composites with complete, uniform nanoscaled silver layer.

In the present study, a facile, convenient and more efficient method for the preparation of mono-dispersed SiO<sub>2</sub>/Ag composite with uniform and complete silver shells was explored. The silica particles were prepared firstly by Stöber process [16]. Then the mixture of polyvinylpyrrolidone stabilized Ag nuclei and the surplus [Ag(NH<sub>3</sub>)<sub>2</sub>]<sup>+</sup> ions was adsorbed on the surface of the silica microspheres. At last, the SiO<sub>2</sub>/Ag composite particles were formed by a simple reduction process in the presence of sodium borohydride (NaBH<sub>4</sub>). All the reactions were carried out at ambient temperature. From the viewpoint of further applications, the photocatalytic activity of SiO<sub>2</sub>/Ag composites was evaluated in the degradation of methyl orange (MO) under visible light irradiation.

## 2. Experimental

### 2.1. Materials

Polyvinylpyrrolidone (PVP, with an average molar mass of 55000 g·mol<sup>-1</sup>), silver nitrate

\*E-mail: zgwu@live.nuc.edu.cn

(AgNO<sub>3</sub>), absolute ethanol (EtOH), tetraethoxysilane (TEOS), sodium borohydride (NaBH<sub>4</sub>), methyl orange (MO) were supplied by Sigma-Aldrich Company. All chemicals and reagents were used as received without further purification. Home-made Milli-Q water was used.

## 2.2. Preparation of SiO<sub>2</sub> microspheres

Silica microspheres were prepared by hydrolysis and polycondensation of TEOS following Stöber method. In a typical experiment, a 50.0 mL ethanol solution containing 4.5 mL TEOS was added to a 16 mL ethanol solution containing 9 mL ammonia and 24 mL H<sub>2</sub>O. The mixture was stirred at room temperature for 3 h with a stirring speed of 300 rpm. The resulting silica microspheres were centrifugally separated from the suspension and then ultrasonically washed with water and ethanol for three times separately. At last, they were dried in an oven at 60 °C for 12 h.

## 2.3. Preparation of silica-silver core-shell composites

Briefly, about 0.3 mL 0.14 M freshly prepared NaBH<sub>4</sub> aqueous solution was dropped into 140 mL aqueous solution containing 0.12 g PVP and [Ag(NH<sub>3</sub>)<sub>2</sub>]<sup>+</sup> (0.1 M) which was produced by the addition of ammonia to AgNO<sub>3</sub> solution. In a separate beaker, 0.025 g of the as-prepared silica microspheres was dispersed in 10 mL deionized water by sonication and it was quickly added into the formerly prepared mixture with vigorous magnetic stirring. Subsequently, 50 mL of 0.14 M NaBH<sub>4</sub> solution, as reducing agent, was dropped at a rate of 0.5 mL/min into the suspensions under stirring. After that the solution was allowed to react for 24 h at room temperature. The solution gradually changed to dark color, indicating the formation of Ag nanoparticles. Finally, the resulting composites were collected by centrifugation, washed with ethanol and dried at 60 °C in a vacuum oven for 12 h.

## 2.4. Characterization

### 2.4.1. Physical analysis

The morphology and dimensions of the products were examined with a high-resolution scanning electron microscope (SEM, JEOL JEM-3000) operated at 20 kV. The compositional information was obtained with an energy-dispersive spectrometer (EDX) installed on SEM. The crystallographic structures of the samples were studied using X-ray diffraction (XRD, Shimadzu XRD6000) with CuK $\alpha$  radiation ( $\lambda = 1.5418 \text{ \AA}$ ) and a scanning range ( $2\theta$ ) of 10° to 80°. UV-Vis absorption spectra were recorded by Scinco S4100 spectrophotometer and all the samples were diluted with ethanol for the measurement. Zeta potential was measured using a Zetasizer 3000HSA setup (Malvern Instruments) equipped with a He-Ne laser (50 mW, 632 nm). The zeta potential measurement based on laser Doppler interferometry was used to measure the electrophoretic mobility of particles. Measurements were performed for 20 s using a standard capillary electrophoresis cell. The dielectric constant was set to 80.4, and the Smoluchowski constant  $F(Ka)$  was 1.5.

### 2.4.2. Photocatalytic property of SiO<sub>2</sub>/Ag composites

The photocatalytic performance of SiO<sub>2</sub>/Ag core-shell composites was measured by the photocatalytic decomposition of organic dye methyl orange (MO) under visible light irradiation at ambient conditions. The experiments were conducted with 20 mg of SiO<sub>2</sub>/Ag composite suspended in 20 mL of MO aqueous solution (10 mg·L<sup>-1</sup>). The solution was pre-stirred in dark for 30 min to establish adsorption-desorption equilibrium. Then, the solutions were exposed to a visible light source (wavelength approximately: 400 nm to 700 nm, 55 W/cm<sup>2</sup>) to irradiate the suspension under stirring. The catalytic performance of the core-shell composites was analyzed quantitatively for the absorption peak at 464 nm of MO in aqueous heterogeneous solution suspensions. The visible-light photocatalytic performance of prepared bare SiO<sub>2</sub> particles was also tested for the photocatalytic degradation of MO under the same conditions.

### 3. Results and discussion

#### 3.1. Characterization of the SiO<sub>2</sub>/Ag composites

##### 3.1.1. XRD analysis

The wide-angle X-ray diffraction (XRD) patterns of the obtained SiO<sub>2</sub> microspheres and SiO<sub>2</sub>/Ag composites are illustrated in Fig. 1. For pure silica particles, there is only a broad scattering maximum centered at 22.5°, corresponding to amorphous silica [15, 17]. Yet, for core-shell composites, except amorphous silica characteristic diffraction peak, it also exhibits four well-resolved diffraction peaks at 2θ angles of 37.9°, 44.1°, 64.3° and 77.2° in the range of approximately 10° to 80°, which can be indexed to the (1 1 1), (2 0 0), (2 2 0), and (3 1 1) reflections of face-centered cubic metal silver (JCPDS Card No. 87-0720), indicating that the Ag nanoparticles with high crystallinity could be obtained on the surface of SiO<sub>2</sub>. In addition, we also can find that the peaks are a little broader than that of bulk silver because the silver grain size is relatively small.

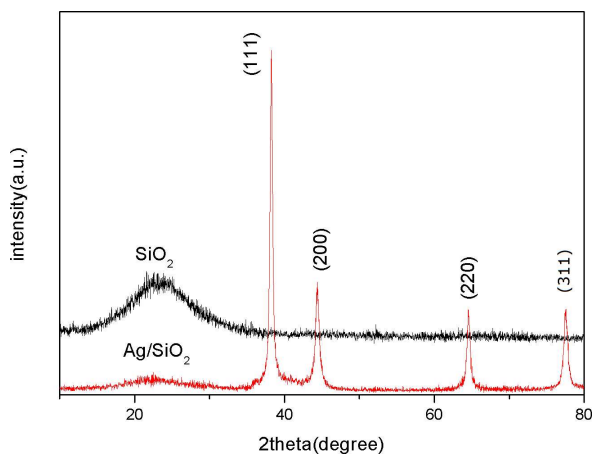


Fig. 1. X-ray diffraction patterns of SiO<sub>2</sub> and Ag/SiO<sub>2</sub> composites.

##### 3.1.2. EDX-SEM

The chemical composition of resulting SiO<sub>2</sub>/Ag composite has been analyzed by EDX elemental analysis as shown in Fig. 2. In this pattern, only Si, O, and Ag peaks are clearly shown and no other peaks are detected. The atomic ratio of Si and O

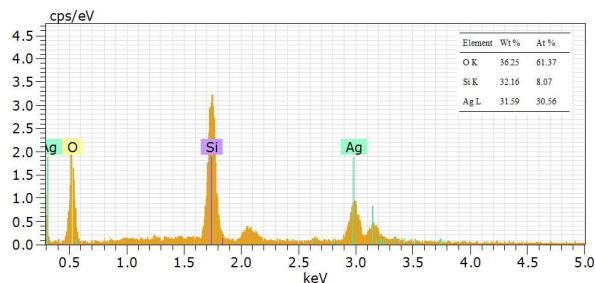


Fig. 2. EDX spectrum of the obtained Ag/SiO<sub>2</sub> composite.

is about 1:2, and the total content of Ag element is about 32 wt.%. This means that the silver shell with high purity has been obtained on the silica microspheres in the present study.

##### 3.1.3. SEM images

SEM images of as-prepared silica microspheres with smooth surface and homogeneous size are shown in Fig. 3a. All of the particles are spherical in shape and the average diameter is about 390 nm. For the core-shell composites shown in Fig. 3b, the silica spheres have been completely covered by consecutive silver nanoparticles. The continuously distributed silver nanoparticles covered the silica surface completely to form a silver shell due to their quite high filling factor on the silica surface. Furthermore, the dispersed composite particles in SEM remained spherical in shape.

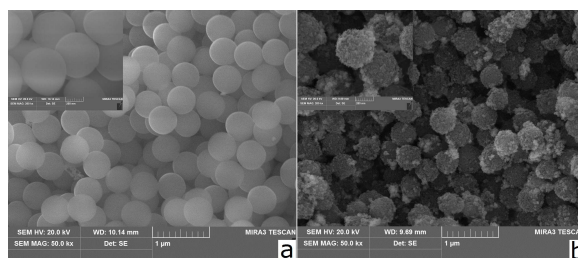


Fig. 3. SEM images of (a) SiO<sub>2</sub> and (b) Ag/SiO<sub>2</sub> composites.

##### 3.1.4. UV-Vis spectroscopy analysis

The UV-Vis spectroscopy is one of the most widely used techniques for structural characterization of silver nanostructures [18, 19]. The absorption spectra of the prepared bare silica and

core-shell structure are shown in Fig. 4. The bare silica colloids do not show any UV-Vis absorption in the range of 300 nm to 800 nm, but the core-shell composites show an obvious absorption peak at around 418 nm due to the Mie plasmon resonance excitation from the silver nanoparticles on the surface of SiO<sub>2</sub>. Compared to pure Ag NPs, the absorption peak shifts from ~400 nm to 418 nm [20, 21]. The possible reason for the red shift can be attributed to much larger size of silver nanoparticles and higher coverage on the silica surface as indicated in Fig. 3b (SEM). The results are consistent with the previous reports [18, 19, 22, 23]. The strong dipole-dipole interactions between neighboring nanoparticles and Mie scattering of silver shell would promote red shift and broadening of the plasmon bands for silver clusters attached on silica spheres.

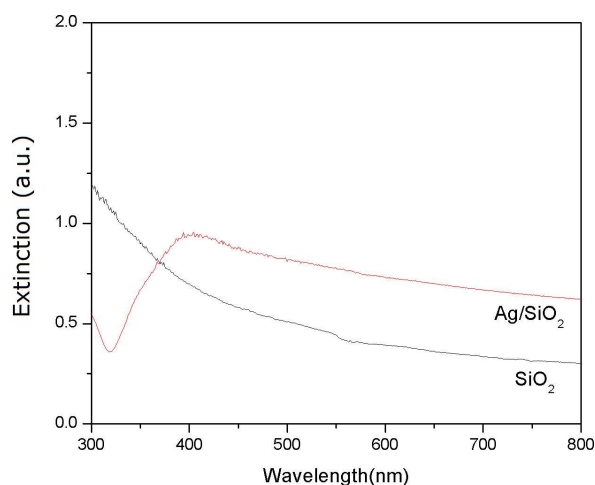


Fig. 4. UV-Vis absorption spectra of SiO<sub>2</sub> and Ag/SiO<sub>2</sub> composites.

### 3.2. Synthetic mechanism of SiO<sub>2</sub>/Ag composites

Fig. 5 describes the mechanism of fabrication of the SiO<sub>2</sub>/Ag core-shell composites. In the first step, because the amount of NaBH<sub>4</sub> is inadequate, both PVP stabilized Ag nuclei (zeta potential ~ +2.3 mV) and surplus [Ag(NH<sub>3</sub>)<sub>2</sub>]<sup>+</sup> ions are existing in the mixture. After the addition of silica microspheres, PVP stabilized Ag nuclei and surplus [Ag(NH<sub>3</sub>)<sub>2</sub>]<sup>+</sup> ions are adsorbed on the surface

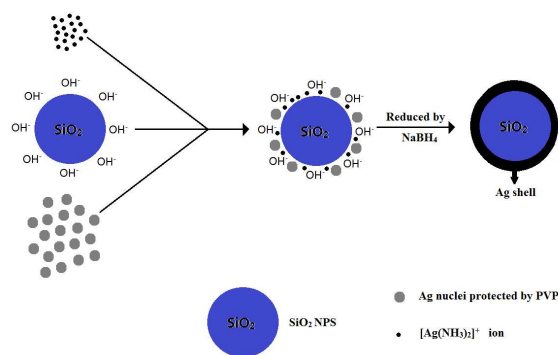


Fig. 5. A simple sketch for the fabrication of SiO<sub>2</sub>/Ag core-shell composites.

of the silica spheres (zeta potential ~ -2.3 mV) via chemisorption and electrostatic attraction [12, 24, 25]. After that, when additional NaBH<sub>4</sub> is dropped into, the reduction process would be initiated. In this process, [Ag(NH<sub>3</sub>)<sub>2</sub>]<sup>+</sup> ions adsorbed on the surface of silica spheres are reduced to Ag nanoparticles. The newly reduced Ag and PVP stabilized Ag nuclei conjugated on the silica surface act as the seeds which provide nucleation sites for the new growth of silver shell [18, 26]. The remaining [Ag(NH<sub>3</sub>)<sub>2</sub>]<sup>+</sup> ions in the solution are further reduced by NaBH<sub>4</sub> and Ag nanoparticles grown gradually on the surface of SiO<sub>2</sub>, eventually lead to the formation of completely covered silver-coated silica spheres.

### 3.3. Photocatalytic degradation analysis of SiO<sub>2</sub>/Ag composites

The photocatalytic activities of the SiO<sub>2</sub>/Ag composites have been investigated by the degradation of methyl orange (MO) under visible light. Pure SiO<sub>2</sub> microspheres have been used for comparison.

The photodegradation dynamic curves of the MO dye are displayed in Fig. 6, in which C<sub>0</sub> represents the initial concentration of MO and C represents the concentration at a given time. As can be seen in Fig. 6, more than 80 % MO dye can be decomposed within 30 min and eventually degraded completely after 60 min with the assistance of SiO<sub>2</sub>/Ag composites under the visible-light irradiation, indicating the excellent photocatalytic

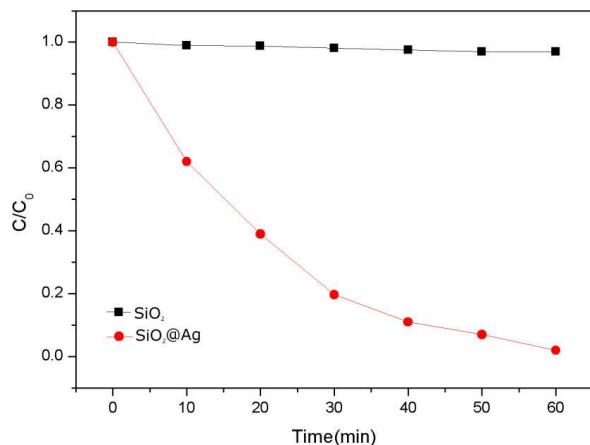


Fig. 6.  $C/C_0$  versus irradiation time plots for MO photodegradation.

activity of the as-prepared core-shell composites, while the photodecomposition ability of pure  $\text{SiO}_2$  microspheres almost can be ignored during the same time interval.

## 4. Conclusions

In summary, we have demonstrated a relatively mild and facile route for the formation of  $\text{SiO}_2/\text{Ag}$  core-shell composites. Their microstructure, chemical composition, optical properties, visible light-driven photocatalytic performance were investigated. The results of XRD, SEM showed that the surface of  $\text{SiO}_2$  was completely surrounded by pure silver nanoparticles, and the silver nanoparticles had fcc structure. With MO degradation efficiency, the  $\text{SiO}_2/\text{Ag}$  composites demonstrated excellent photocatalytic activity.

## References

- [1] CHEN K.H., PU Y.C., CHANG K.D., LIANG Y.F., LIU C.M., YE H.J.W., SHIH H.C., HSU Y.J., *J. Phys. Chem. C*, 116 (2012), 19039.
- [2] ATWATER H.A., POLMAN A., *Nat. Mater.*, 9 (2010), 205.
- [3] JANKIEWICZ B.J., JAMIOLA D., CHOMA J., JARONIEC M., *Adv. Colloid Interfac.*, 170 (2012), 28.
- [4] PHADTARE S., KUMAR A., VINOD V.P., DASH C., PALASKAR D.V., RPA M., SHUKLA P.G., SIVARAM S., SASTRY M., *Chem. Mater.*, 15 (2003), 1944.
- [5] WEI S.Y., WANG Q., SHU J.H., SUN L.Y., LIN H.F., GUO Z.H., *Nanoscale*, 3 (2011), 4474.
- [6] PAN K.Y., LIANG Y.F., PU Y.C., HSU Y.J., YE H.J.W., SHIH H.C., *Appl. Surf. Sci.*, 311 (2014), 399.
- [7] GU G.X., XU J.X., WU Y.F., CHEN M., WU L.M., *J. Colloid Interf. Sci.*, 359 (2011), 327.
- [8] HUANG J., WANG H.T., ZHANG K.S., *Desalination*, 336 (2014), 8.
- [9] WANG M., XU X.F., MA B., PEI Y.Y., AI C.C., YUAN L.J., *RSC Adv.*, 4 (2014), 47781.
- [10] PARK S.J., DUNCAN T.V., SANCHEZ-GAYTAN B.L., PARK S.J., *J. Phys. Chem. C*, 112 (2008), 11205.
- [11] LIU T., LI D.S., YANG D.R., JIANG M.H., *Colloid. Surface. A*, 387 (2011), 17.
- [12] FLORES J.C., TORRES V., POPA M., CRESPO D., CALDERÓN-MORENO J.M., *J. Nanosci. Nanotechnol.*, 9 (2009), 3177.
- [13] JIANG Z.J., LIU C.Y., LIU Y., ZHANG Z.Y., LI Y.J., *Chem. Lett.*, 32 (2003), 668.
- [14] JONI I.M., BALGIS R., OGI T., IWAKI T., OKUYUMA K., *Colloid Surface A*, 388 (2011), 49.
- [15] ZHANG Q.S., YE J.W., TIAN P., LU X.Y., LIN Y., ZHAO Q., NING G.L., *RSC Adv.*, 3 (2013), 9739.
- [16] STÖBER W., FINK A., BOHN E., *J. Colloid Interf. Sci.*, 26 (1968), 62.
- [17] LIOU T.H., CHANG F.W., LO J.J., *Ind. Eng. Chem. Res.*, 36 (1997), 568.
- [18] TANG S.C., TANG Y.F., ZHU S.P., LU H.M., MENG X.K., *J. Solid State Chem.*, 180 (2007), 2871.
- [19] JIANG Z.J., LIU C.Y., *J. Phys. Chem. B*, 107 (2003), 12411.
- [20] KHAN Z., AL-THABAITI S.A., OBAID A.Y., AL-YOUBI A.O., *Colloid. Surface. B*, 82 (2011), 513.
- [21] STEINIGEWEG D., SCHLÜCKER S., *Chem. Commun.*, 48 (2012), 8682.
- [22] XU C., LI W.J., WEI Y.M., CUI X.Y., *Mater. Design*, 83 (2015), 745.
- [23] XIU Z.L., WU Y.Z., HAO X.P., ZHANG L., *Colloid. Surface. A*, 386 (2011), 135.
- [24] KIM Y.H., LEE D.K., CHA H.G., KIM C.W., KANG Y.S., *J. Phys. Chem. C*, 111 (2007), 3629.
- [25] DENG Z.W., CHEN M., WU L.M., *J. Phys. Chem. C*, 111 (2007), 11692.
- [26] TZOUNIS L., CONTRERAS-CACERES R., SCHEL-LKOPF L., JEHNICHEN D., FISCHER D., CAI C.Z., UHLMANN P., STAMM M., *RSC Adv.*, 4 (2014), 17846.

Received 2016-03-01  
Accepted 2016-10-20